Electronic Supplementary Material

Highly selective sorting of semiconducting single wall carbon nanotubes exhibiting light emission at telecom wavelengths

Francesco Sarti[1], Francesco Biccari[1], Federica Fioravanti[1], Ughetta Torrini[1], Anna Vinattieri[1], Vincent Derycke[2], Massimo Gurioli[1], and Arianna Filoramo[2] (✉)

[1] Department of Physics and LENS, University of Florence, Via Sansone 1, 50019 Sesto Fiorentino, Italy
[2] LICSEN, NIMBE, CEA, CNRS, University Paris-Saclay, CEA Saclay, 91191 Gif sur Yvette CEDEX, France

S1 Raman spectra

Typical Raman spectra of the A samples are reported in Fig. S1. Green and red lines refer to the $S_{3,3}$ and $M_{1,1}$ resonant excitations (see the inset of Fig. S1(a)), respectively (the two spectra have been offset for a better comparison). Raman spectra were collected by a T64000 Jobin-Yvon spectrometer (in triple configuration) through an optical microscope (Olympus BX41, objective 100×), the excitation source was either a single longitudinal mode (SLM) laser emitting at 660 nm (Torus 660 Laser Quantum) or SLM laser emitting at 514.5 nm (Fandango Cobolt); the spot size was about 1 μm. In all samples a well resolved RBM signal (around 200 cm⁻¹) is found when exciting at $S_{3,3}$ (λ_{exc} = 514.5 nm) but a different behavior is found when exciting at $M_{1,1}$ (λ_{exc} = 660 nm). Signatures of the presence of metallic SWNTs can be found in the Raman spectra of A1, A2, and A4 samples. Conversely no detectable signal from metallic species is observed in the A3 sample where only the signature of polymer is recorded. Note that the Raman spectra have not been smoothed; no subtraction of background has been performed and that the eventual PL contributes to this background.

More specifically, when considering sample A4 we see that even though ultrahigh centrifugation is effective in reducing the presence of bundles in solution, signatures of metallic species are still present in the spectra. Note also that such signatures are generally hardly detectable in the absorption spectra (as reported in Fig. 1(c)) and here we benefit from the resonance enhancement of Raman spectroscopy. Thus, we conclude that for A1, A2, and A4 the used speed/time is not sufficient to remove completely the metallic species. We suggest that the strong sonication used for sample A4 has actually favored also the suspension of isolated metallic nanotubes (or very small bundles containing some metallic nanotubes) which was counterproductive when compared with A3. Note also that the D band at about 1,350 cm⁻¹, which is due to the presence of defect assisted scattering [S1, S2], is dependent on the processing, denoting that an improved dispersion favors the removal of the detrimental amorphous phase.

Address correspondence to arianna.filoramo@cea.fr

We suggest also that the difference in the Raman signal intensities of A1/A2 samples with respect to A3/A4 ones is related to the presence of nanotubes bundles in the solutions when high speed ultracentrifugation step is not performed. In this case nanotubes bundles containing even a single metallic nanotube do not contribute to PL signal. The contribution due to scattering with the polymer is present in the spectra, too. For A3/A4 samples this contribution could be enhanced by the high speed ultracentrifugation since the final nanotube concentration is reduced while the polymer concentration is unchanged.
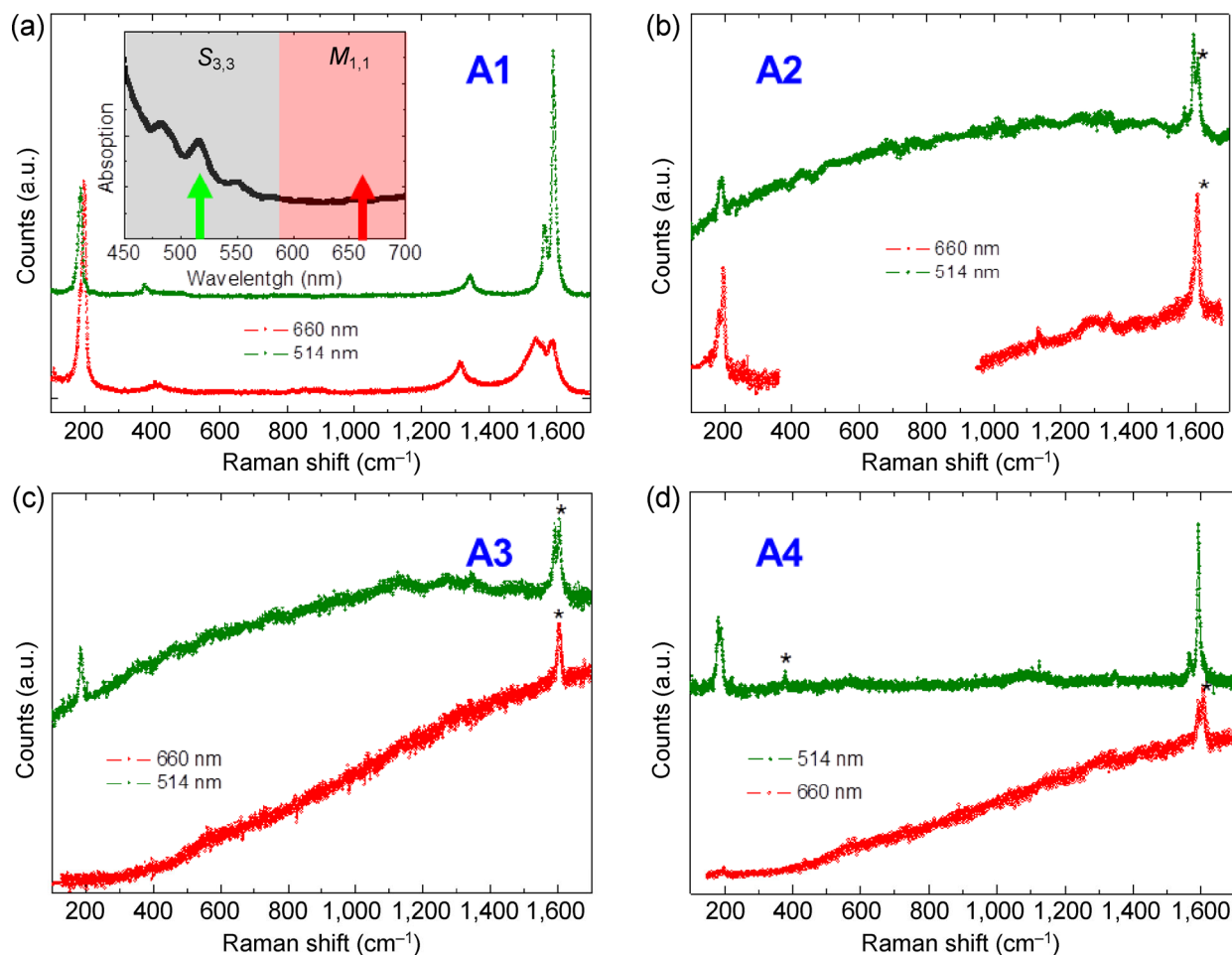

Figure S1 Inset of (a) comparison of the absorption spectrum with the excitation wavelengths used for Raman. (a)–(d) Raman spectra of the samples A1, A2, A3, and A4. In order to observe selectively only semiconductor or metallic nanotubes, two different wavelengths of the excitation laser were used: Red curves correspond to 660 nm excitation (for m-SWNTs) whereas green curves correspond to 514.5 nm excitation (for s-SWNTs). The small stars correspond to the Raman signal of the residual PFH-A.

S2   Absorption spectroscopy

We performed the experiment using PFH-A and larger diameter nanotube (arc discharge) too. Using the same process parameters (of samples A1, A2, A3, and A4) we obtain very similar results, as reported in Fig. S2. Note that the fundamental transitions for this type of nanotubes are out of the region of interest for telecom wavelengths.
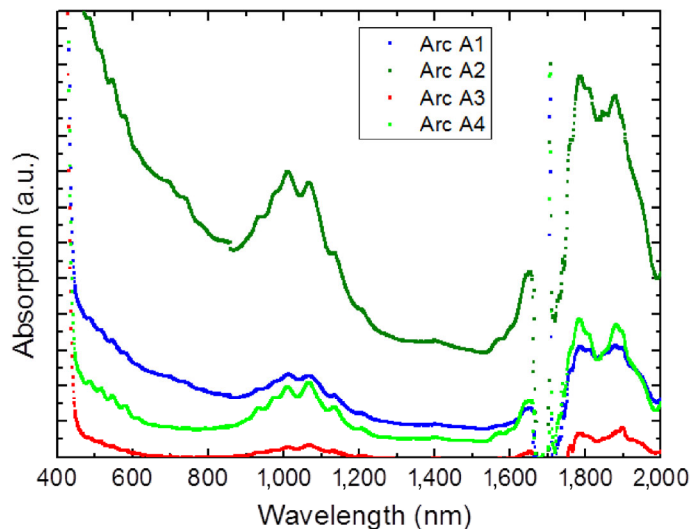
Figure S2 Absorption as a function of wavelength for solution prepared using arc discharge nanotubes and PFH-A following the protocol of A1, A2, A3, and A4 samples. The noisy region around 1,650–1,750 nm is related to the solvent.

S3   AFM images

AFM images of the surface after SWNT deposition by spin coating and washing by toluene and acetone. The AFM images reported in Fig. S3 concern the deposition of solution to check washing out of PFH-A polymer from the SWNTs and form the substrate surface. Even if few traces of polymer can be found, the SWNT are clearly observed in the AFM. The AFM images reported in Fig. S4 show the surface of devices after SWNTs deposition and washing process. Here SWNTs are bridging two contacts.
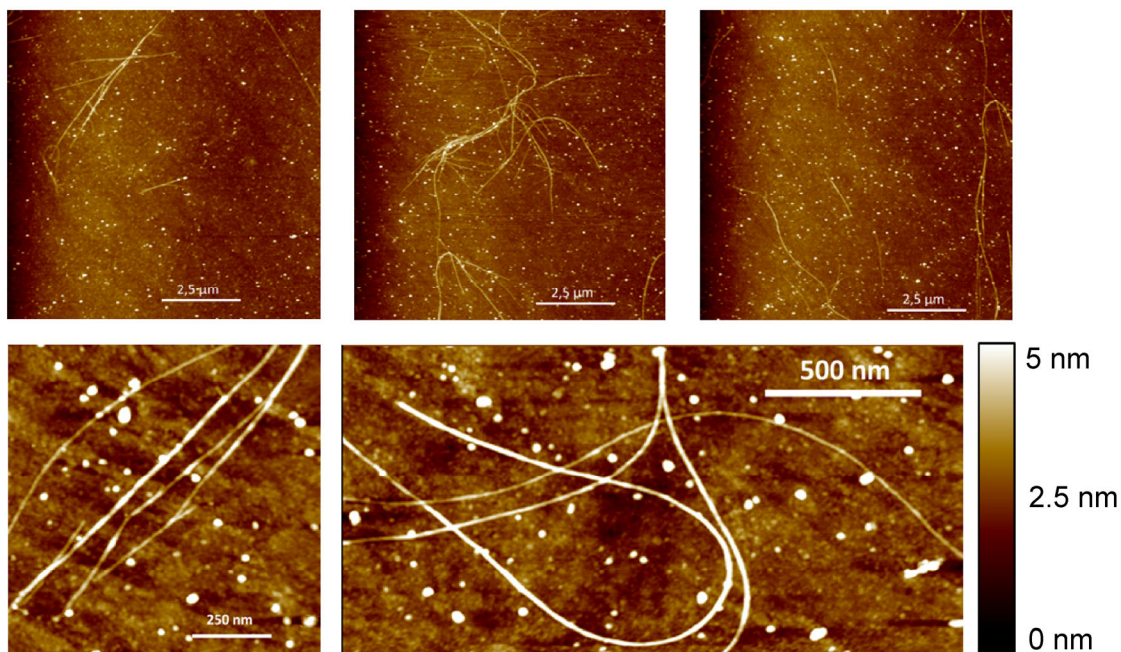

Figure S3 AFM images (height; tapping mode) showing the effect of washing by toluene and acetone. The SWNTs are deposited from the solution onto a Si/SiO$_2$ or quartz substrate and polymer is partially washed out leaving large bare portion of the SWNTs. Trace of polymer are visible onto the surface.
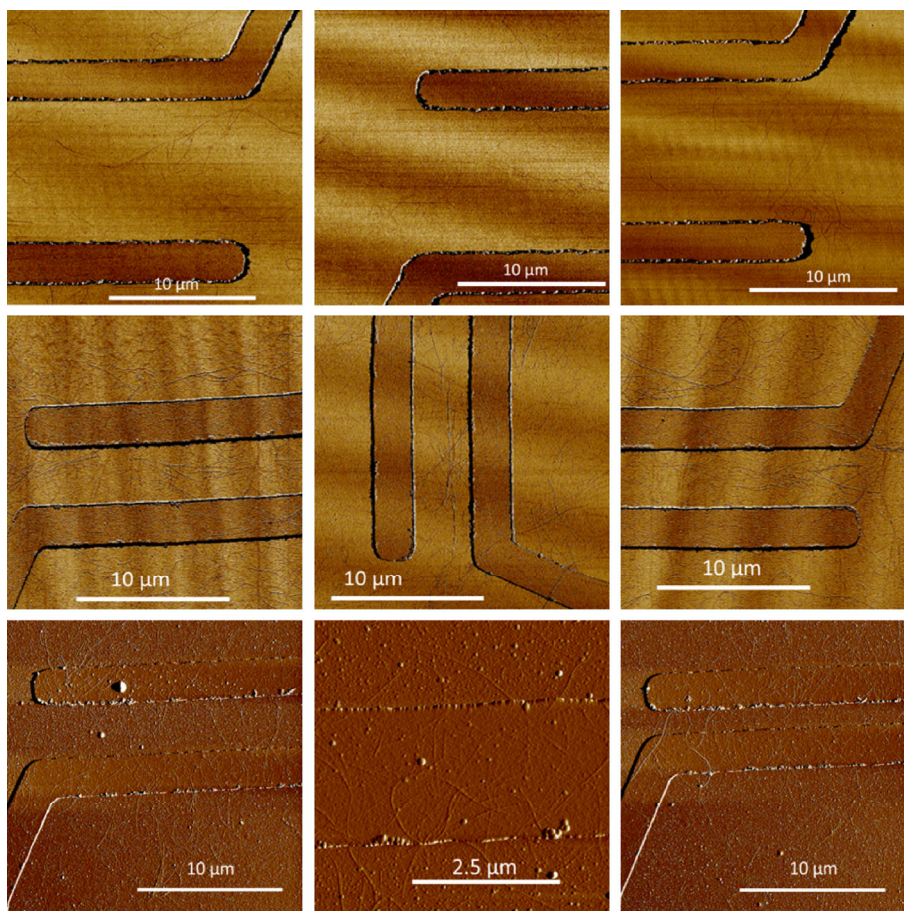
Figure S4 AFM images (phase; tapping mode) showing the effect of washing by toluene and acetone. The SWNTs are deposited from the solution onto a Si/SiO$_2$ with pre-patterned electrodes and then polymer is partially washed out. Traces of polymer are visible onto the surface.

References

[S1] Thomsen, C.; Reich, S. Double resonant Raman scattering in graphite. *Phys. Rev. Lett.* **2000**, *85*, 5214–5217.

[S2] Thomsen, C.; Reich, S. Raman scattering in carbon nanotubes. In *Light Scattering in Solids IX: Novel Materials and Techniques*. Cardona, M.; Merlin, R., Eds.; Springer-Verlag: Berlin Heidelberg, 2007; pp 115–232.